Morphology transitions at vicinal Cu surfaces based on entropic step-step interaction and diffusion along steps

Heike Emmerich
Max-Planck-Institut für Physik komplexer Systeme, Nöthnitzer Str. 38, D-01187 Dresden, Germany
(Received 25 July 2001; revised manuscript received 7 February 2002; published 4 June 2002)

An extension of the Burton-Cabrera-Frank model including diffusion along steps and entropic step-step interaction is introduced. This extended model is successfully applied to simulate recent experiments at vicinal Cu surfaces [T. Maroutian *et al.*, Phys. Rev. Lett. **83**, 4353 (1999)]. In particular, the rise of two qualitatively different morphologies can be explained by the competition of the four distinct driving and restoring forces of the model implying different directions for the growth of instabilities along the step edges. In addition, a linear stability analysis of the extended model is carried out. The result is a wavelength for the fastest growing mode which is larger than the one predicted by Bales and Zangwill and in agreement with the experiments.

DOI: 10.1103/PhysRevB.65.233406 PACS number(s): 68.35.Rh, 68.35.Fx

During molecular beam epitaxy (MBE) appropriate conditions for the controlled growth of vicinal surfaces can be fine tuned and one can fabricate either atomistically flat or nanostructured surfaces. The ability to exert control on structuring along the growth direction and fabricate substrates with smallest-scale built-in periodicities normal to the surface is well advanced. Efforts to better determine functional properties of a grown substrate now focus on the lateral structuring within one layer of growth. One direction along this line is to make use of the inherent instabilities due to the dynamics of the growth process itself.[1] A necessary first step is to understand the basic wavelengths of those inherent instabilities in addition to the kind of morphologies which will develop.

More then ten years ago, Bales and Zangwill[2] predicted that a growing vicinal surface should undergo a step meandering instability when kinetic step-edge barriers suppress the attachments of atoms to descending steps.[3] According to their analysis, a straight step is linearly unstable against perturbations with wavelengths larger than $\lambda_c = 2\pi\sqrt{2\Gamma L_\Delta}$ and a fastest growing wavelength at $\lambda_u = \sqrt{2}\lambda_c$ ($\Gamma = \Omega\gamma/k_BT$, $L_\Delta = Dc^0_{eq}/Fl^2$). Here F denotes the deposition rate, D the diffusion constant for diffusion *on* the terraces, c^0_{eq} the equilibrium concentration of a straight step, γ the step stiffness, Ω the atomic area, and k_BT the thermal energy. Even though the meandering instability has meanwhile been observed in experiments and simulations,[4] the quantitative prediction of the Bales-Zangwill analysis could not be recovered in many of those experimental findings. This point received much interest in view of recent experiments by Maroutian *et al.*[5] at CEA Saclay. Analytical efforts to resolve the disagreement between experimental measurements and theoretical prediction led to a precise study of the limit of desorptionless growth. To derive a single evolution equation this case has the interesting feature of displaying a singularity in the spirit of multiscale expansion.[6] As a result, meander wavelengths larger than the ones predicted by Bales and Zangwill can be explained, however, without reaching the order of experimental observations.[7] Other efforts center around the investigation of an extra diffusion current *along* step edges.[8] Such a current triggers an asymmetry in energy barriers for atoms attaching at kinks from different step-edge directions, the so-called kink Ehrlich-Schwoebel effect (KESE).[9,10] The KESE can either destabilize or stabilize steps depending on whether the slope of the meander instability is greater or less than 1. In Ref. 5 calculations including a stabilizing KESE current along steps were compared to the further conjecture that islands might nucleate at step edges and thereby constitute a still different wavelength of instability. It appeared that including this assumption produced a better fit to the experimental wavelength values.

A different light was shed on these investigations by experiments which revealed that a morphology qualitatively different from the meandering one can develop on a vicinal surface as well, with growth conditions being exactly the same as for the meandering morphology except for a different polar angle of the vicinal.[11] This morphology can be characterized by the absence of one global growth direction and thereby resembles the so-called *degenerated morphology*.[12] Thus the inadequacy of theoretical approaches to explain the difference between the wavelength of instability predicted by Bales and Zangwill and the one observed experimentally was further revealed by the failure to explain this *degenerated morphology*. Note that the surface of the in-phase meandering morphology displayed in the scanning tunnel microscope (STM) topograph in their Fig. 1(b) (Ref. 5) was wrongly identified as Cu(1,1,17) and is in fact a Cu(0,2,24) surface. The true Cu(1,1,17), on the other hand, displays a *degenerated morphology*.[11]

In this paper I will introduce a different model which can explain the rise of two different morphologies as well as their basic wavelengths including KESE currents plus entropic step-step repulsion in the classical Burton-Cabrera-Frank (BCF) model.[13] It is the competition between the destabilizing and the stabilizing forces combined in this extended BCF model (EBCF model) which results into two different kinds of morphologies depending on the difference in magnitude of orthogonal driving forces. In contrast to the widely used Monte Carlo models[19,20] for the simulation of vicinal surface growth, as a continuum model the EBCF allows for a mathematical stability analysis. This reveals an analytical expression for the basic wavelength of the meander instability which is in agreement with recent experimental observations.

Moreover, careful investigations with the model elucidate the fact, that to explain (i) the correct morphology transitions *plus* (ii) the correct wavelength formation at Cu vicinals, all four of the driving and restoring forces explained underneath in detail have to be taken into consideration. This model resolves these four physical components as well as the dynamics resulting from their interaction explicitly.

To get an impression of the basic ideas underlying the EBCF model let us start with the one-sided BCF model, i.e., the model formulated by Burton, Cabrera, and Frank in 1951 for the case of complete suppression of attachment of adatoms to descending steps. This one-sided BCF model constitutes a *moving boundary problem* of a diffusion-relaxation equation for the dynamics of the adatoms on the terraces and two boundary conditions for the conservation of mass and the conservation of energy at the steps, respectively:

$$\partial_t c = D\nabla^2 c - \frac{1}{\tau} c + F, \tag{1}$$

$$c_{eq} = c_{eq}^0 \cdot (1 + \kappa \Omega \tilde{\gamma} / k_B T), \tag{2}$$

$$v_n = D\Omega \frac{\partial c}{\partial n}. \tag{3}$$

Here c and κ denote the areal adatom density and the step curvature, respectively. $\tilde{\gamma}$ refers to the step stiffness taking into account its fourfold anisotropy. Equations (2) and (3) are to be evaluated at the front of each step. For vicinal Cu surfaces in the temperature range of the experiments under discussion a current involving the diffusion coefficient D_m along the kinked steps is operative.[8] Following the notation of Pierre-Louis *et al.* in Ref. 10 this diffusion along steps plus its anisotropy due to KESE can be included in the *moving boundary problem* above by adding $-\partial_x J_k$ to the right-hand side of Eq. (3), where J_k refers to the KESE current given by Eqs. (2) and (3) of Ref. 10. For a meandering step with local slope $|M|>1$ it reads

$$J_k = \frac{F_s^{\perp}(1-|M|)M}{L_s + |M|}, \tag{4}$$

where L_s denotes the KESE length and $F_s^{\perp}$ the respective incident flux. J_k is a function of the local slope of the meandering step with respect to the straight step. Since growth proceeds in the direction of minimal step stiffness, the initial orientation of the meandering instability is aligned with this direction of minimal step stiffness. Assuming the step edges to be infinitesimal sections of a surface perpendicular to (001), the orientational dependency of the step stiffness can be determined in direct analogy to the calculation of variations of surface tension with surface orientation in Ref. 14. The appropriate potential is a Lennard-Jones potential. The result is the $\langle 130 \rangle$ orientation of edges as the direction to minimize step stiffness. This implies that this direction of minimal step stiffness encloses an angle θ_0 of approximately 63.5° with the straight steps in case of Cu(1,1,17), whereas θ_0 is approximately 71.5° in the case of Cu(0,2,24). θ_0 has to be taken into account as part of $\tilde{\gamma}$, i.e.,

$$\tilde{\gamma} = \tilde{\gamma}_0[1 - \epsilon_4 \cos(\theta - \theta_0)], \tag{5}$$

where $\tilde{\gamma}_0$ refers to the step stiffness of a straight step, ϵ_4 to the material's crystalline anisotropy and θ to the angle between the normal vector of a straight step and the local normal of the meandering step. With an initial orientation of instabilities in the $\langle 130 \rangle$ direction, destabilizing J_k currents of different magnitudes are triggered with respect to a straight step direction in either $\langle 110 \rangle$ or $\langle 100 \rangle$. To evaluate J_k a quantitative value for the KESE length L_s is required. The diffusion barrier for the jump of a single adatom along the step edge in the $\langle 130 \rangle$ direction is ~ 0.39 eV picturing it as an alternation of one jump with a barrier of 0.26 eV succeeded by one jump with barrier of 0.52 eV according to Ref. 19. From this the KESE length L_s can be derived as 0.2016×10^3. The resulting j_k current densities for Cu(0,2,24) versus Cu(1,1,17) differ by one order of magnitude: for Cu(0,2,24) j_k takes a value of 3.5518×10^{-7} $(\text{Å s})^{-1}$, whereas for Cu(1,1,17) $j_k = 3.1915 \times 10^{-8}$ $(\text{Å s})^{-1}$. Despite their different magnitudes in both cases KESE currents are destabilizing, favoring unsaturating amplitude growth. Wavelengths of instabilities turn out to be even less than in the BCF model. As a consequence, taking into account KESE as the only additional driving force in the BCF model cannot explain the experimental work by T. Maroutian and co-authors. An obvious antagonist of the destabilizing KESE is the repulsion due to the succeeding step. Entropic as well as elastic interactions[16] have to be taken into account. Since the step interaction energy A is small compared to the entropic repulsion in the temperature ranges under discussion[15], it is sufficient to extend Eq. (2) by taking into account the suppression of step wandering:

$$c_{eq} = c_{eq}^0 + \frac{\kappa}{k_B T} \cdot \left(\Omega \tilde{\gamma} c_{eq}^0 + \frac{(\pi k_B T)^2}{6 l^2 \tilde{\gamma}} \right), \tag{2'}$$

$$v_n = D\Omega \frac{\partial c}{\partial n} - \partial_x J. \tag{3'}$$

The additional term $(\pi k_B T)^2 / 6 l^2 \tilde{\gamma}$ is the step interaction parameter with l the width of the terraces. Equations (1), (2′), and (3′) constitute the extended BCF model (EBCF). Its simulation with $T = 280$ K, $F = 3 \times 10^{-3}$ monolayers/s, $l = 21.7$ Å, $D_m = 10^{-6}$ cm^2/s, $c_{eq}^0 = 8.208 \times 10^{-6}$ Å^{-1}, and $\tilde{\gamma} = 1.034$ eV/Å yields two morphologies for the Cu(0,2,24) surface (Fig. 1) and the Cu(1,1,17) (Fig. 2), respectively (no desorption).

The four components regulating growth of instabilities in the EBCF model are:

(i) enhancement of growth via the gradient of the adatom diffusion field normal to the interface setting the length scale L_Δ as a primary wavelength of the meandering instability;

(ii) restore via step stiffness (corr. length scale: Γ);

(iii) driving of amplitude growth via KESE (scale: L_s);

(iv) restore via entropic repulsion (scale: $L_S = 6\gamma l^2 / k_B T \pi^2$) .

In the situation depicted by Fig. 2 the magnitude of the KESE current derivative $\partial_x J$ is negligibly small. The remain-

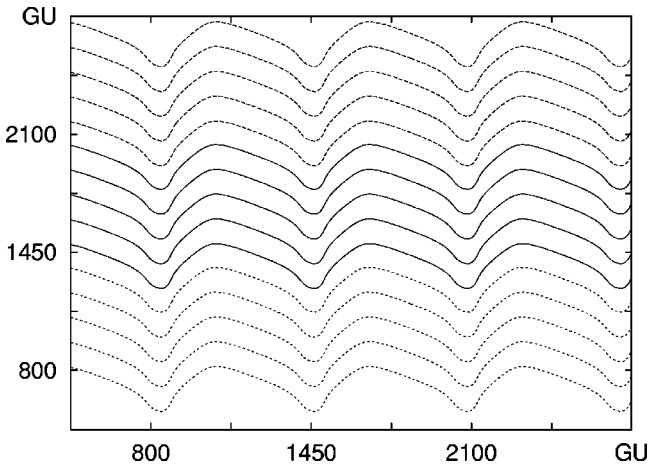

FIG. 1. In-phase meandering according to numerical simulations of the EBCF model. The parameters of the simulation are calibrated to Fig. 1(b) in Ref. 5. GU refers to grid units of the underlying numerical grid. A train of 15 steps with periodic boundary conditions in the lateral direction is displayed. Horizontal boundary conditions are periodic as well. Space calibration leads to roughly ten grid units corresponding to 1 Å. Asymmetry with respect to the *y* axis is a consequence of θ_0 in Eq. (5).

ing forces due to entropic and step stiffness effects act in directions perpendicular to each other. The result of this competition of perpendicular forces of equal strength is the *degenerated morphology* as observed in other contexts with an analogous competition of driving forces.[12]

In Fig. 1 the KESE current contributes to the evolution of surface morphology. It has a component which is opposed to the entropic forces reducing their overall effect. The magnitude of the remaining driving force due to this KESE current is ten times smaller then the magnitude of the adatom diffusion field gradient in the direction of minimal step stiffness. The precise factor, evaluated via the simulation, is 11.129 for Fig. 1 averaged over 500 time steps. Due to the dominance of L_Δ, growth can proceed in the direction of minimal step stiffness.

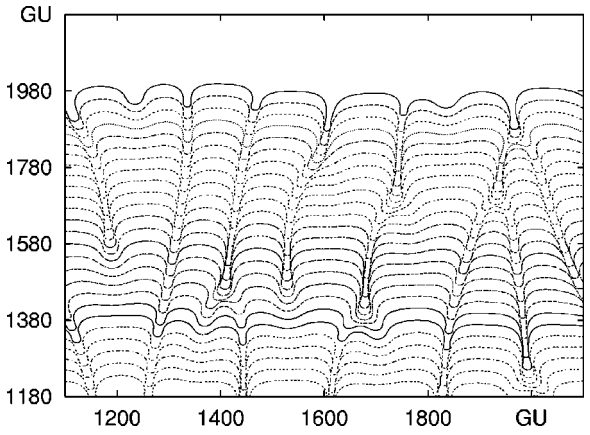

FIG. 2. The *degenerated* morphology as obtained in simulations. Same as in Fig. 1 except a different scale of 1 GU corresponding to 1 Å and taking into account the different vicinal [namely Cu(1,1,17) versus Cu(0,2,24)] via a different angle between the alignment of straight steps and the direction of minimal step stiffness (i.e., θ_0). A train of 25 steps with the first step growing towards infinity is displayed. This simulation result is in good agreement with the *degenerated* morphology recorded for Cu(1,1,17) after deposition of about 20 monolayers (ML's) at $F=5\times10^{-3}$ ML's/s at surface temperature 285 K via STM topography (Ref. 11).

To understand the basic wavelength of the instability the two new length scales L_S and L_s, set by entropic interaction as in Eq. $(2')$ and by an anisotrop diffusion current along the step as in Eq. $(3')$ respectively, have to be taken into account. Equations (1), $(2')$, and $(3')$ constitute a system with a type-I bifurcation.[17] Its dispersion relation can be evaluated in an analogy to a dilute binary alloy undergoing directional solidification[18]. For $\Gamma \ll Ł_S$ the resulting expression to leading order reads

$$\lambda_u = \sqrt{2}\pi\left(\frac{L_\Delta \cdot \Gamma \cdot Ł_S}{4}\right)^{1/3} + 2\sqrt{2}\pi\frac{\Gamma L_s}{3l_T}. \tag{6}$$

Here $l_T = 2D/v_0$, where v_0 denotes the velocity of a straight step. Equation (4) replaces Eq. (1) in Ref. 5. It is sufficient in the most interesting temperature range $2.8\text{–}3.8\times10^{-3}$ K^{-1}, where it displays deviations from an Arrhenius-type behavior, which increases with increasing temperature. Nevertheless, it is in good agreement with the experimental data (Fig. 3). Simulations of the EBCF model also support this expression.

The EBCF model explains two relevant interesting results for growth at vicinal surfaces, namely the experimentally observed deviation from the Bales-Zangwill instability and

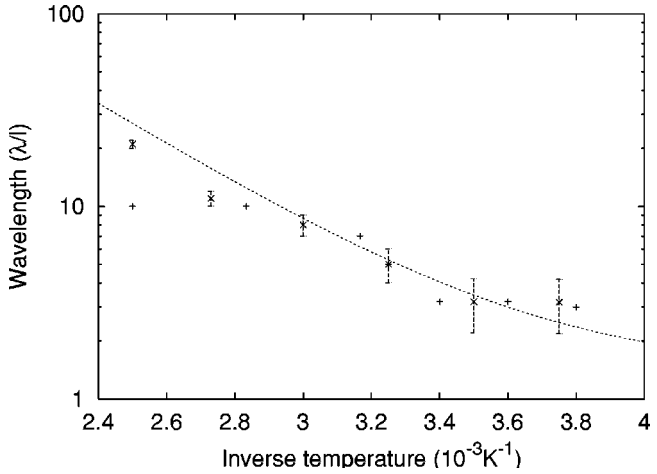

FIG. 3. The "+" data points are taken from Ref. 5 and give the wavelength measurements recorded there. The dashed line is the solution of Eq. (4). Crosses with error bars are data points obtained from simulation with the EBCF. There are limitations to a precise wavelength measure in simulations. Due to the horizontal periodic boundary conditions wavelengths are always a divider of the system's width. Enlarging this system width systematically until the rise of a further cell as well as restricting the width until the extinction of one of the cells allows the determination of upper and lower bounds. Data points are the mean of these bounds which themselves are taken into account via the error bars, thus each data point is a result of up to 15 simulations with different system widths.

the rise of a *degenerated morphology*. I am not aware of any other model which allows for an analytical wavelength analysis as well as for a quantitative investigation of the morphology transition via explicit consideration of all four competing driving and restoring forces discussed here. These results are related to experimental findings in the group of H.-J. Ernst. The new basic wavelength predicted theoretically from the EBCF model can be observed as initial perturbation of the step at the Cu(0,2,24) as well as the Cu(1,1,17) surfaces. The qualitative difference between their morphologies, i.e., whether a surface displays an in-phase-meandering [Cu(0,2,24)] or a *degenerated* structure [Cu(1,1,17)] after deposition of a few monolayers, depends on the magnitude of the angle between the direction of destabilizing and restoring forces. Time scales for the development from initial perturbation to the full *degenerated* morphology could not be compared with experiments due to the lack of experimental data. It seems an interesting question whether *in situ* transitions from one morphology to the other can be obtained via a change in the ratio of driving forces (e.g., by lowering temperature during the experiment). Whether this morphology transition displays features which resemble a true phase transition remains to be investigated.

The diffusion relaxation Eq. (1) is solved on a quadratic grid. The interface is discretized separately by curvilinear segments and respective interpolations from the interface to the grid.

I thank T. Maroutian for sending me a STM picture of the true Cu(1,1,17) surface morphology as well as M. Rusanen for sending me Ref. 20 prior to publication. Comments by H. Müller-Krumbhaar as well as assistance by T. Ihle when getting started on explicit solvers for moving boundary problems are gratefully acknowledged.

[1] J.-K. Zuo and J. F. Wendelken, Phys. Rev. Lett. **78**, 2791 (1997); H.-J. Ernst *et al.*, *ibid.* **72**, 112 (1994); L. C. Jorritsma *et al.*, *ibid.* **78**, 911 (1997); J. A. Stroscio *et al.*, *ibid.* **75**, 4246 (1997); J. E. Van Nostrand *et al.*, *ibid.* **74**, 1127 (1995).

[2] G. S. Bales and A. Zangwill, Phys. Rev. B **41**, 5500 (1990).

[3] R. L. Schwoebel and E. J. Shipsey, J. Appl. Phys. **37**, 3682 (1966).

[4] L. Schwenger, R. L. Folkerts, H.-J. Ernst, Phys. Rev. B **55**, R7406 (1997); J. E. Van Nostrand, S. J. Chey, and D. G. Cahill, *ibid.* **57**, 12 536 (1998); P. Tejedor, P. Šmilauer, and B. A. Joyce, Microelectron. J. **30**, 477 (1999); M. Rost, P. Šmilauer, and J. Krug, Surf. Sci. **369**, 393 (1996); H. Emmerich *et al.*, J. Phys.: Condens. Matter **11**, 9985 (1999).

[5] T. Maroutian, L. Douillard, and H.-J. Ernst, Phys. Rev. Lett. **83**, 4353 (1999).

[6] O. Pierre-Louis *et al.*, Phys. Rev. Lett. **80**, 4221 (1998).

[7] J. Kallunki and J. Krug, Phys. Rev. E **62**, 6229 (2000).

[8] M. Giesen-Seibert *et al.*, Phys. Rev. Lett. **71**, 3521 (1993); **23**, 911(E) (1994); Surf. Sci. **329**, 47 (1995); K. Mussawisade, T. Wichmann, and K. W. Kehr, *ibid.* **412/413**, 55 (1998).

[9] I. L. Aleiner and R. A. Suris, Fiz. Tverd. Tela **34**, 1522 (1992) [Sov. Phys. Solid State **34**, 809 (1992)]; Z. Zhang and M. G. Lagally, Science **276**, 377 (1997); J. G. Amar, Bull. Am. Phys. Soc. **43**, 851 (1998).

[10] O. Pierre-Louis, M. R. D'Orsogna, and T. L. Einstein, Phys. Rev. Lett. **82**, 3661 (1999).

[11] T. Maroutian, L. Douillard, and H.-J. Ernst, Phys. Rev. B **64**, 165401 (2001).

[12] F. Heslot and A. Libchaber, Phys. Scr. **T9**, 126 (1985); S. Akamatsu, G. Faivre, and T. Ihle, Phys. Rev. E **51**, 4751 (1995).

[13] W. K. Burton, N. Cabrera, and F. C. Frank, Philos. Trans. R. Soc. London, Ser. A **243**, 299 (1951).

[14] D. Wolf, Surf. Sci. **226**, 389 (1990).

[15] H.-C. Jeong and E. D. Williams, Surf. Sci. **171**, 47 (1999), and references therein.

[16] B. Houchmandzadeh and C. Misbah, J. Phys. I **5**, 685 (1995); C. Duport, P. Politi, and J. Villain, *ibid.* **5**, 1371 (1995).

[17] M. C. Cross and P. C. Hohenberg, Rev. Mod. Phys. **65**, 851 (1993).

[18] W. W. Mullins and R. F. Sekerka, J. Appl. Phys. **35**, 444 (1964).

[19] M. Rusanen, I. T. Koponen, J. Heinonen, and T. Ala-Nissila, Phys. Rev. Lett. **86**, 5317 (2001), and references therein.

[20] Y. Saito and M. Uwaha, Phys. Rev. B **49**, 10 677 (1994); S. Schinzer *et al.*, *ibid.* **60**, 2893 (1999); I. Furman *et al.*, *ibid.* **62**, R10 649 (2000).